ACS APPLIED MATERIALS & INTERFACES

Research Article

www.acsami.org

Surface-Initiated Atom Transfer Radical Polymerization-Induced Transformation of Selenium Nanowires into Copper Selenide@Polystyrene Core–Shell Nanowires

Michael C. P. Wang and Byron D. Gates*,†

†Department of Chemistry and 4D LABS, Simon Fraser University, 8888 University Drive, Burnaby, British Columbia V5A 1S6, Canada

Supporting Information

ABSTRACT: This Article reports the first preparation of cuprous and cupric selenide nanowires coated with a ~5 nm thick sheath of polystyrene (copper selenide@polystyrene). These hybrid nanostructures are prepared by the transformation of selenium nanowires in a one-pot reaction, which is performed under ambient conditions. The composition, purity, and crystallinity of the copper selenide@polystyrene products were assessed by scanning transmission electron microscopy, electron energy-loss spectroscopy, X-ray powder diffraction, and X-ray photoelectron spectroscopy techniques. We determined that the single crystalline selenium nanowires are converted into polycrystalline copper selenide@polystyrene nanowires containing both cuprous selenide and cupric selenide. The product is purified through the selective removal of residual, non-transformed selenium nanowires by performing thermal evaporation below the decomposition temperature of these copper selenides. Powder X-ray diffraction of the purified copper selenide nanowires@polystyrene identified the presence of hexagonal, cubic, and orthorhombic phases of copper selenide. These purified cuprous and cupric selenide@polystyrene nanowires have an indirect bandgap of 1.44 eV, as determined by UV–vis absorption spectroscopy. This new synthesis of polymer-encapsulated nanoscale materials may provide a method for preparing other complex hybrid nanostructures.

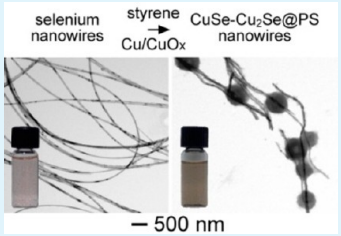

KEYWORDS: *selenium, copper selenide@polystyrene, core–shell nanowire, solid–solid reaction, template-engaged synthesis, atom transfer radical polymerization*

INTRODUCTION

A significant research effort has been put into studying copper selenides because they have a wide range of applications in fields that include gas sensing,[1] thermal electrics,[2] nonlinear optics,[3] therapeutics,[4] and photovoltaics.[5] Researchers have been recently focusing on synthesizing copper selenide nanostructures with controlled shapes and sizes to tune their optoelectronic properties.[1,6−17] Copper selenides are a desirable material for photovoltaic applications because they can be easily doped with other metals to enhance their solar conversion efficiency.[18,19] In addition, recent studies have shown that copper selenide nanostructures could be useful in photothermal therapy because these materials are both less expensive and have superior photothermal efficiencies in contrast to gold nanostructures.[4] However, metal chalcogenides have not been widely adopted in theranostics applications because of their lethality in biological systems.[20] It is desirable to passivate the copper selenides with a material that would prevent the dissolution of these toxic substances *in vivo*. In addition, the passivating layer can be tailored with the appropriate functional group(s) to increase the colloidal stability of the nanostructure in various media, making the material easier to handle and process for subsequent steps such as device integration or assembly. Polymer encapsulation of nanowires has been shown to increase the corrosion resistance and ease of handling of the core material.[21] Polymer encapsulated copper selenide nanowires could, therefore, be less lethal in biological systems when used in theranostics applications and may improve their stability and ease of processing for other applications. There are, however, no previous demonstrations of coating copper selenide nanostructures with a thin encapsulating sheath of polymer.

Herein, we report a method to synthesize copper selenide nanowires that are simultaneously encapsulated with a thin layer of polystyrene (PS) by surface-initiated atom transfer radical polymerization (SI-ATRP). This process is demonstrated using selenium nanowires dispersed in styrene in the presence of a copper substrate covered with a native oxide. X-ray photoelectron spectroscopy suggested that styrene radicals facilitated the reduction of copper(II) species to copper(I) and copper(0) and that both of which reacted spontaneously with the selenium nanowire templates to produce cuprous (Cu_2Se) and cupric selenide (CuSe) nanowires.

There are many synthetic approaches to make copper selenide nanostructures. One of the most commonly reported procedures relies on the coreduction of either salts or

Received: June 19, 2013
Accepted: September 1, 2013
Published: September 2, 2013

   dx.doi.org/10.1021/am4023785 | ACS Appl. Mater. Interfaces 2013, 5, 9546–9553

organometallic precursors of copper and selenium in the presence of solvated ligands.[6,7,15] Most of these reports have focused on the synthesis of 0D,[7] 2D, or 3D nanostructures of copper selenides, such as triangular or hexagonal plates,[7] discs,[6] and cubes.[15] Another approach is to transform amorphous and crystalline selenium structures into copper selenide crystals by the mutual diffusion of copper and selenium atoms. Two-dimensional copper selenide ribbons and discs have been prepared at room temperature by a solid-state chemical reaction between thin films or particles of selenium and copper deposited on top of each other under vacuum.[22−28]

In general, there have been fewer articles published on the synthesis of 1D nanostructures of copper selenide. One-dimensional copper selenide nanostructures have been synthesized by both solution-phase and gas-phase techniques.[1,2,9−11,13] High-aspect-ratio copper selenide nanowires can be grown under vacuum through chemical vapor deposition (CVD), but this technique requires a careful choice of precursors.[9] Low-aspect-ratio copper selenide nanorods have been electrochemically grown within the pores of an anodized alumina membrane.[10,13] This electrodeposition method can easily yield anisotropic nanostructures, but the technique is limited by low throughput in comparison to more easily scalable solution-based syntheses. Some solution-phase syntheses can produce 1D copper selenide nanostructures with both an increased aspect ratio and an increased yield. One approach to the solution-based synthesis of 1D copper selenide nanostructures uses hydrothermal and solvothermal techniques.[1,2,11] These syntheses can be performed in the absence of surfactants that are commonly used to promote the anisotropic growth of metallic 1D nanostructures.[29,30] A preformed structural template can also guide the formation of copper selenide nanorods in solution, as Alivisatos et al. demonstrated through the use of cadmium selenide nanorods with diameters below 10 nm.[12] This reaction involved the exchange of cations that reside within the nanorod template (i.e., Cd(II)) with the desired cation (i.e., Cu(II)). This template-engaged route to copper selenide is limited by the ion-exchange process and diffusion kinetics within the solid material, which restricts the ability to synthesize copper selenide nanostructures of larger diameters without the use of high temperatures. As an alternative approach, Yang et al. reported the synthesis of copper selenide nanotubes from a template of trigonal selenium nanotubes.[16] In their synthesis, a mild reducing agent was used to convert Cu(II) into Cu(I), which reacted spontaneously with the Se(0) nanotubes to produce copper selenide nanotubes in an aqueous environment.

In this Article, we report a template-engaged method to directly convert selenium nanowires into polystyrene-encapsulated cuprous and cupric selenide core−shell (CuSe-Cu_2Se@PS) nanowires. This transformation occurs under ambient conditions via a series of reactions initiated by atom transfer radical polymerization. CuSe-Cu_2Se@PS has the potential of being corrosion resistant, similar to *t*-Se@PS.[21] Scanning transmission electron microscopy, electron energy-loss spectroscopy, X-ray powder diffraction, and X-ray photoelectron spectroscopy techniques are used to characterize the composition, purity, and crystallinity of the CuSe-Cu_2Se@PS products. The bandgap of the CuSe-Cu_2Se@PS was determined by UV−vis absorption spectroscopy.

EXPERIMENTAL SECTION

Copper selenide nanowires were synthesized from templates of selenium nanowires. These sacrificial selenium nanowires were grown by solution-phase techniques following the Ostwald ripening of amorphous selenium colloids via a sonication-induced solvothermal process.

Synthesis of Selenium Nanowires.[21] Amorphous selenium was prepared by first dissolving 2.73 g (21.1 mmol) of selenious acid (H_2SeO_3, 98%; Sigma-Aldrich) in 100 mL of 18.2 MΩ·cm water (purified using a Barnstead NANOpure DIamond Life Science water filtration system) contained within a 250 mL round-bottomed glass flask. This solution was cooled in an ice-water bath for 20 min before introducing the reducing agent hydrazine (N_2H_4, 50−60% in water; Sigma-Aldrich). An ice-water chilled solution of hydrazine, 3 mL (61.1 mmol), was introduced drop-by-drop into the reaction solution under constant magnetic stirring over a period of 2 min. After 15 min of continuous stirring, the brick-red precipitate was collected by vacuum filtration onto a PVDF membrane with an average pore size of 0.1 μm (Millipore no. VVLP04700). The filtrate was rinsed with 200 mL of 18.2 MΩ·cm water to remove residual N_2H_4. The resulting red solid was stored in a plastic petri dish wrapped in aluminum foil and freeze dried in a Savant Modulyo lyophilizer (Thermo Scientific) at −50 °C and 100 mbar for 12 h. This red solid was characterized as amorphous selenium particles by XRD and elemental analysis.

A solvochemical route was used to synthesize the selenium nanowires from the amorphous selenium particles. In brief, a dispersion containing 1 mg of amorphous selenium powder in 2 mL of ethanol (EtOH, 95%; Commercial Alcohols) dispersed in a 2 dram glass vial was sonicated for 20 s. The solution was then placed in a dark cabinet maintained at 22 °C to allow the reaction to reach completion over a period of ∼12 h.

Synthesis and Purification of Copper Selenide@Polystyrene Nanowires. An ethanol solution containing selenium nanowires was drop cast onto a piece of copper plate (∼0.5 cm × 1 cm^2) coated with a layer of native oxide. Ethanol was evaporated under vacuum, leaving a dried sample of selenium nanowires on the copper substrate. Subsequently, the copper substrate with selenium nanowires was placed in a 5 mL screw-capped glass vial containing 1.5 mL of styrene, which had been passed through an alumina column to filter off the chemical inhibitors in the solution. The reaction vial was kept at room temperature under ambient light. The progress of the transformation into copper selenide@polystyrene was initially monitored by observing the slow transformation of the dark-red selenium nanowires into black copper selenide nanowires.

The crude product dispersed in styrene was collected by decanting, isolated by centrifugation at 3000 rpm for 5 min, and rinsed with EtOH. This purification procedure was performed a total of three times to remove residual styrene. A solution of ethanol containing the crude product, which consisted of a mixture of cuprous and cupric selenide@polystyrene and selenium nanowires, was transferred to a Schlenk tube. The solvent was subsequently removed under vacuum. To remove selectively the excess starting material (unreacted selenium nanowires), the Schlenk tube (fitted with a cold finger) was heated at 300 °C for 12 h. Thermal evaporation under vacuum to remove residual selenium nanowires was performed with a similar set up with the side-arm of the Schlenk tube coupled to the vacuum gas manifold of a Schlenk line. The Schlenk line was coupled to a Welch® DuoSeal® (Model 1400) vacuum pump. The sample was heated at 160 °C for 12 h under vacuum. Evaporated selenium collected onto the cold finger located above the sample. The purified product was redispersed in ethanol.

Materials Characterization Techniques. Scanning electron microscopy (SEM) images and energy-dispersive X-ray spectroscopy (EDS) data were acquired with an FEI Strata DB235 FESEM operating at 15 kV. Samples for SEM analysis were prepared by drop casting a solution of nanowires onto a piece of approximately 1 cm^2 silicon wafer. Transmission electron microscopy (TEM) images, energy-dispersive X-ray spectroscopy (EDS), and selected area electron diffraction (SAED) data were obtained with either an FEI

Tecnai G^2 F20 scanning TEM (STEM) with a field emission gun thermionic source operating at 200 kV or a Hitachi 8000 STEM with a lanthanum hexaboride thermionic source operating at 200 kV. Analysis by electron energy loss spectroscopy (EELS) was carried on the Tecnai G^2 F20 STEM equipped with a Gatan GIF 2000 imaging filter. The spectrometer had an energy resolution of 1.1 eV that was calculated from the full-width at half-maximum of the zero loss peak obtained with a 2 mm aperture and a detector setting of 0.1 eV/channel. For TEM and EELS analysis, the samples were prepared by drop-casting or dip-coating solutions of nanowires onto a 300 mesh copper grid coated with formvar/carbon (Cedarlane Laboratories Ltd. no. FCF300-CU-50) or onto a Quantifoil holey carbon copper grid (Cedarlane Laboratories Ltd. no. Q225-CS7). Nickel TEM grids coated with silicon monoxide (Soquelec International no. D20515) and carbon (Electron Microscopy Sciences no. CF-150-Ni) were used in the STEM−EDS analysis for the elemental composition of the copper selenide nanostructures.

X-ray diffraction (XRD) patterns were acquired with a Rigaku diffractometer using Cu Kα radiation (λ = 0.15418 nm). Copper X-rays were generated from a copper target by electron bombardment at 42 kV and 40 mA. A 0.5 mm collimator was placed between the X-ray source and the sample. Samples for X-ray analysis were prepared by casting a suspension of nanowires from EtOH onto a glass slide and drying the sample under vacuum.

Optical absorption measurements (UV−vis spectroscopy) were performed with a Varian Cary 300 Bio spectrophotometer system. Samples of nanowires were dispersed into ethanol contained within a 1 cm path length quartz cell (type 100-QS, Hellma Analytics no. 100-10-40). Each solution of nanowires was sonicated for 30 s to achieve a uniformly dispersed solution prior to acquiring the optical absorption measurements. It is crucial to obtain a uniform dispersion to minimize scattering of incident radiation.

X-ray photoelectron spectroscopy (XPS) analysis was carried out on a Kratos Analytical Axis Ultra DLD spectrometer using a monochromatic aluminum source (Al Kα, 1486.6 eV) operating at 150 W (10 mA emission current and 15 kV HT), with the exception that the aluminum source was operated at 75 W (5 mA emission current and 15 kV HT) when analyzing the polystyrene films to minimize sample charging. Analyses were conducted on a 700 × 300 μm^2 area of the samples. High-resolution scans were obtained at a 50 meV step size with a dwell time of 1000 ms per step and a pass energy of 20 eV. The Kratos charge neutralizer was used during analysis of insulating samples. Energy scale linearity was calibrated using Al and Mg X-ray sources on Argon sputter-cleaned gold and copper substrates. The calibration procedure was performed in accordance with ISO 15472 international procedure. XPS analyses were performed on polystyrene (Aldrich, M_w ca. 280 000 by GPC), CuSe-Cu_2Se@PS, a copper substrate prior to the surface-initiated atom transfer radical polymerization, as well as a copper substrate that has been used to convert selenium nanowires into cuprous and cupric selenide@polystyrene nanowires. All spectra have been calibrated with respect to the peak position of the C−C signal of C1s at 284.6 eV. Vision 2 Processing software (version 2.2.7) was used to analyze and perform curve fitting on the XPS spectra.

RESULTS AND DISCUSSION

Copper selenide nanowires encapsulated in a sheath of polystyrene (CuSe-Cu_2Se@PS) are synthesized from selenium nanowires. The selenium nanowires transform into copper selenide by a series of reactions initiated by the formation of styrene free radicals. Monomers of styrene are converted to free radicals either by exposure to heat or UV irradiation.[31] These free radicals of styrene are able to reduce some of the Cu(II) species on the surfaces of a Cu/CuOx substrate to Cu(I) species, as indicated by X-ray photoelectron spectroscopy (XPS) analysis (Supporting Information Figure S1a,c). It has been documented that Cu(I) species react spontaneously with selenium to produce cuprous selenide (Cu_2Se).[16,32] The concentration of Cu(0) at the surface increased for a Cu/CuOx substrate that had been immersed in styrene in comparison to a Cu/CuOx sample spectrum acquired in the absence of styrene. This result suggests that styrene radicals are capable of reducing Cu(II) species into Cu(0). Prior literature reports that selenium particles in physical contact with Cu(0) undergo a solid-state reaction to produce cupric selenide (CuSe) by the mutual diffusion of Cu and Se atoms.[22,23,26] Scanning electron microscopy (SEM) analysis revealed that the surfaces of the Cu/CuOx substrate immersed in a mixture of styrene and selenium nanowires became rough. The new structures included discs and ribbons, suggesting the formation of copper selenides (Supporting Information Figure S1b).[22,23,28] In addition, free radicals of styrene would initiate polymerization of styrene monomers to encapsulate both the starting materials[21] and the newly formed copper selenide nanowires. In the absence of styrene, the selenium nanowires and Cu/CuOx substrate did not transform into copper selenide nanowires. Both cuprous and cupric selenide nanowires were not observed by X-ray diffraction (XRD) and transmission electron microscopy (TEM) analyses did not indicate the presence of copper selenide nanowires (Supporting Information Figure S2). Analysis by XPS confirmed the presence of Cu(II) species and an absence of Cu(I) species on the surfaces of Cu substrate (Supporting Information Figure S1c). Moreover, SEM analysis revealed that the surfaces of the Cu substrate had remained unchanged, suggesting that no chemical reaction had occurred (Supporting Information Figure S1d). We believe that a layer of CuO and $Cu(OH)_2$ overlayers on the Cu/CuOx substrate served as a barrier to inhibit the mutual diffusion of Cu and Se atoms.

To synthesize copper selenide@polystyrene nanowires, a sample of selenium nanowires deposited on a Cu/CuOx substrate was immersed into styrene. Transmission electron microscopy analysis (Figure 1a) reveals that the 1D nanostructures of selenium initially have a uniform diameter along their growth direction of [001]. Bend contours along the length of the nanowires can also be observed in the bright-field TEM image. These features are a hallmark of high-aspect-ratio single crystalline 1D nanomaterials. Selected area electron diffraction (SAED) analysis (Figure 1a inset) performed on a single selenium nanowire produced a pattern of diffraction spots that correlates to single-crystal selenium with a hexagonal symmetry. In this case, the collimated electron beam passed through the selenium nanowire perpendicular to the [210] zone axis. After the reaction mixture is left at room temperature under ambient lighting for a period of 3 months, the selenium nanowires and the Cu/CuOx substrate exhibited a noticeable change in their coloration. The nanowires turned dark grey in color, in contrast to the dark brick-red color of the selenium nanowires, whereas the shiny orange-toned Cu/CuOx substrate changed to a dull red. Analysis by TEM (Figure 1b) indicates that the newly formed anisotropic nanostructures have a different morphology than the starting material. These nanowires have non-uniform diameters with multiple bends along the length of the nanowire and are encapsulated in a low-contrasting polystyrene sheath similar to selenium@polystrene nanowires prepared by a surface-initiated atom transfer radical polymerization.[21] X-ray photoelectron spectroscopy was employed to determine the composition of the polymer coating on the copper selenide nanowires. A high-resolution C1s photoemission spectrum of the copper selenide@polystyrene nanowires indicated the presence of a $\pi-\pi^*$

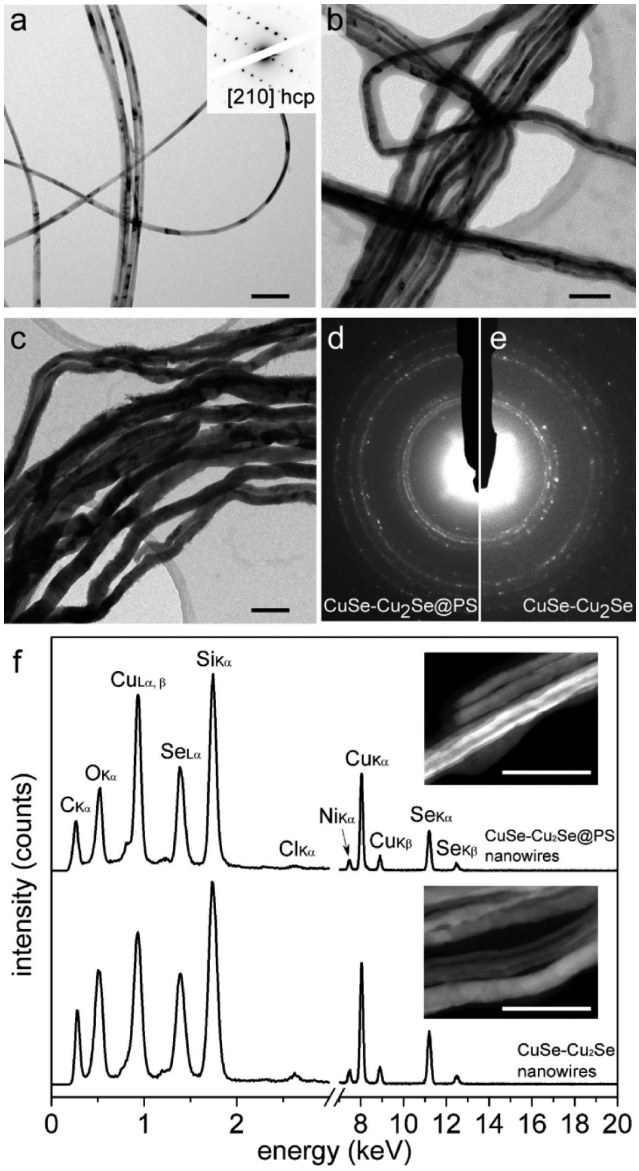

Figure 1. (a, inset) Corresponding transmission electron microscopy (TEM) and selected-area electron diffraction (SAED) pattern of the 1D selenium templates. (b) TEM analysis revealing the presence of a new species of polycrystalline nanowires encapsulated in a low-contrasting material after prolonged incubation of both a Cu substrate and *t*-Se nanowires in a solution of styrene. (c) TEM of copper selenide nanowires without polymer encapsulation formed by reacting Cu(I) species on a Cu substrate with selenium nanowires. (d, e) Electron diffraction patterns of these Cu1.75±0.04Se@PS and Cu1.63±0.04Se nanowires. (f) Elemental analysis by energy dispersive X-ray spectroscopy (EDS) on a scanning transmission electron microscope (STEM) of the polystyrene-encapsulated copper selenide nanowires (top inset) and uncoated copper selenide nanowires (bottom inset) deposited on SiOx-coated Ni grids. Scale bars are 200 nm.

electronic transition that is a signature of unsaturated or aromatic carbon species. This peak corresponds to the phenyl rings of the polystyrene (Supporting Information Figure S3).[33] The thickness of the polystyrene coating is nonuniform along the length of the copper selenide nanowires. Nodules of PS are present along the length of these nanowires (Supporting Information Figure S4). This nonuniformity is attributed to the fact that SI-ATRP was performed at room temperature. The rate of polymerization is proportional to local variation in reactivity along the selenium nanowire templates. Polystyrene colloids produced as a byproduct of the reaction can be removed by isolating the polystyrene-encapsulated copper selenide nanowires via centrifugation at 3000 rpm followed by decanting the supernatant. A higher temperature can be used to accelerate the transformation of selenium to copper selenide nanowires, but the rate of styrene polymerization also increases. The resulting product is a viscous and tacky mass. Copper selenide nanowires without polystyrene encapsulation (Figure 1c) can also be produced by drop casting selenium nanowires onto a Cu(I) and Cu(0) enriched Cu/CuOx substrate (Supporting Information Figure S1a) that had been used to synthesize the polystyrene-coated copper selenide nanowires. This reaction was facilitated by an increase in the surface concentration of Cu(I) and Cu(0) on the Cu/CuOx substrate from the presence of styrene radicals, as indicated by the XPS analysis. The Cu(I) and Cu(0) species on the surfaces of the Cu/CuOx substrate can react with the selenium nanowires by two possible mechanisms. The Cu(I) species on the surfaces of the Cu/CuOx substrate can react electrochemically[16,32] to produce cuprous selenide (Cu2Se). In addition, copper selenides (CuSe and Cu2Se) can be formed through solid-state reactions between Cu(0) and Se(0), as reported in previous literature.[22,23,26,27] The newly formed copper selenide nanowires, both with or without the polymer coating, no longer exhibit the bend contours and have an increased contrast in the TEM images. These changes indicate the formation of a polycrystalline material that has a higher density than selenium. The electron diffraction patterns obtained from multiple copper selenide nanowires indicate similar crystal lattices for nanowires with and without the polymer coating (Figure 1d,e). Elemental analysis by energy dispersive X-ray spectroscopy (EDS) performed by STEM on an area containing a collection of copper selenide nanowires confirmed that these new nanostructures are composed of copper and selenium (Figure 1f). Elemental composition analyses were extracted from these EDS spectra shown in Figure 1f using TEM Imaging & Analysis software provided by FEI Company (version 4.2 SP1). The bare copper selenide nanowires have an average composition of Cu1.63±0.04Se, and the polystyrene-encapsulated copper selenide core−shell nanowires have an average composition of Cu1.75±0.04Se@PS. In addition, spot EDS analyses performed along the length of individual Cu1.75±0.04Se@PS nanowire revealed a larger variation in composition between Cu and Se in comparison to the Cu1.63±0.04Se (Supporting Information Figure S5). Variation in the ratio of Cu/Se observed in Cu1.75±0.04Se@PS nanowires could be due to the formation of the polystyrene layer, which occurs simultaneously to the electrochemical transformation of selenium into copper selenide. The polystyrene coating could impede the selenium nanowires from reacting uniformly with the Cu(I) species or there may be an uneven supply of reactive Cu species along the length of the selenium nanowire because some sections of the nanowire are dispersed in the styrene and not in physical contact with the Cu substrate. Poor physical contact would result in a nonuniform product for a solid-state chemical reaction. These polycrystalline 1D nanostructures have an average core diameter of 76 ± 21 nm (Supporting Information Figure S6), which is ∼2.6 times larger than the average diameter of selenium nanowires at 29 ± 9 nm. Because the copper selenide nanowires retain the anisotropic form of the template nanowires, the mechanism of transformation is

unlikely to proceed solely by reduction of Se(0) into Se^{2-} before it reacts with the reactive copper species. The complete reduction of selenium would have resulted in the formation of copper selenide colloids.[6,7] The reaction may instead have proceeded through an electrochemical process in which Cu(I) ions diffused into the selenium nanowires as well as through a solid state reaction in which Cu(0) atoms diffused into the selenium in contact with the Cu substrate.[16,22−28,32,34] The combination of both processes lead to the transformation of selenium nanowires into cupric and cuprous selenide nanowires.

Copper selenide and copper selenide@polystyrene nanowires were further investigated with alternative TEM imaging modes to analyze the crystalline domains within these nanostructures. Under higher magnification TEM in the bright-field imaging mode (Figure 2a,c) in which the (000) diffraction spot is used to acquire the image, features such as grain boundaries and Moiré fringes are easily identifiable. The specific size of each grain and the orientation of these grains are difficult to discern from the bright-field image. Different regions of the sample that have similar crystal orientations and therefore jointly contribute to specific electron beam diffractions can be distinguished using a dark-field imaging mode. For example, other individual diffraction spots can be used to produce an image that distinguishes the size and distribution of grains within the Cu1.75±0.04Se@PS and Cu1.63±0.04Se nanowires that contribute to this diffraction (Figure 2b,d). This analysis suggests that the crystalline domains within the copper selenide nanowire have lateral dimensions from approximately 2 to 50 nm. Additional confirmation of the phase and purity of copper selenide nanowires was sought using X-ray spectroscopy.

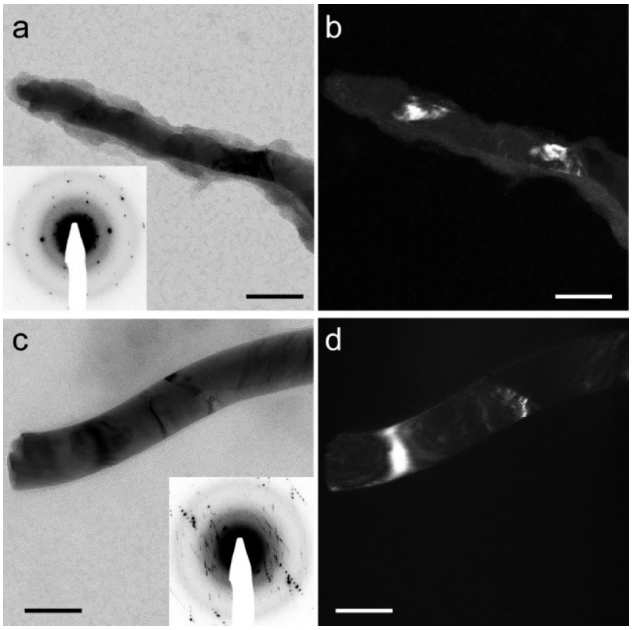

Figure 2. (a, c) Grain boundaries and Moiré fringes are observable in a bright-field TEM image of a copper selenide@polystyrene nanowire (CuSe-Cu_2Se@PS NW) and copper selenide nanowire (CuSe-Cu_2Se NW), respectively, obtained using the (000) diffraction spot. (b, d). Dark-field images acquired from the same region of each sample reveal the size and frequency of grains within each nanowire that have a similar orientation to one another. Scale bars are 100 nm.

We investigated the phase of the anisotropic copper selenide by powder XRD analysis. The acquired diffraction pattern (Supporting Information Figure S7) contains a set of overlapping diffraction peaks. Some of these diffractions arise from unreacted selenium nanowires, which correlate to PDF no. 42-1245. Other peaks coincide with hexagonal copper selenide (CuSe, PDF no. 01-072-8417 34-171), cubic copper selenide (Cu2Se, PDF no. 46-1129), and orthorhombic copper selenide (CuSe, PDF no. 86-1239). After 1 month of reaction, the reaction product consists of ∼43% copper selenide nanowires and ∼57% selenium nanowires.

The presence of selenium nanowires in the product diminishes with increasing reaction time. After 3 months, ∼97% of selenium nanowires were converted to copper selenide nanowires. The powder XRD pattern was studied by a quantitative Rietveld phase analysis (Supporting Information Figure S8) through a Materials Analysis Using Diffraction (MAUD) program.[35] Optical characterization of the as-synthesized nanowires, such as by UV−vis absorption spectroscopy, could lead to an erroneous interpretation of the electronic transitions of the copper selenide nanowires. Therefore, the unreacted selenium nanowires must be selectively removed from the sample. Selenium can be dissolved in a number of solvents, such as hydrazine[36] and carbon disulfide,[37] but these chemicals might also influence the composition of the copper selenide nanowires. Hence, an alternative method of was sought to selectively remove residual selenium from the as-synthesized mixture.

Differential scanning calorimetry studies of selenium and copper selenide indicate these materials have very different melting and decomposition temperatures. Selenium melts at 221 °C,[38] whereas the copper selenide decomposes to β-Cu2-XSe at 380 °C.[14] By operating between these two temperature ranges, it is possible to selectively remove the unreacted Se from the crude product by thermal evaporation. One method of purification is to heat a batch of crude product at 300 °C in a Schlenk tube fitted with a cold finger under ambient pressure for 12 h. Subsequent analysis of the heat-treated samples by powder XRD (Figure 3) indicates the selective removal of

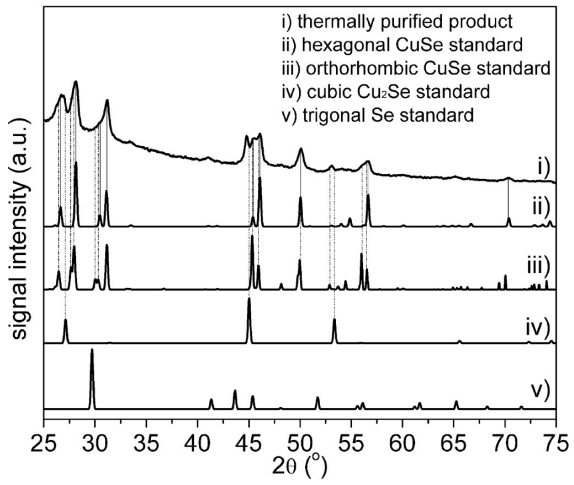

Figure 3. X-ray diffraction pattern depicting a sample of purified nanowires after the successful removal of selenium from the crude product by heating the sample at 300 °C for 12 h. The pure copper selenide nanowires consist of a mixture of hexagonal (PDF no. 01-072-8417 34-171), orthorhombic (PDF no. 86-1239), and cubic (PDF no. 46-1129) phases.

dx.doi.org/10.1021/am4023785 | ACS Appl. Mater. Interfaces 2013, 5, 9546−9553

selenium nanowires from the crude product because of the absence of trigonal selenium (*t*-Se) diffraction peaks. Heating the PS beyond its decomposition temperature[39] would lead to carbonization of the polymer, converting the PS coating on the copper selenide nanowires into a mixture of amorphous carbon and graphite. High-angle annular dark-field (HAADF) imaging through scanning transmission electron microscopy analysis of the copper selenide@polystyrene nanowires revealed a change in the density of the PS coating after the sample had been thermal purified (Supporting Information Figure S9). Prior to thermal purification to remove residual selenium nanowires, the PS coatings had a relatively low contrast (Supporting Information Figure S9a, inset). These low-contrast coatings were also observed in the STEM images of thermally purified copper selenide@polystyrene nanowires, which were purified either at 300 °C under atmospheric pressure or under vacuum at 160 °C (Supporting Information, insets of Figure S9b and S9c, respectively). Analysis by XPS of these purified samples revealed the absence of the $\pi-\pi^*$ transition at ~291 eV, indicating that the polymer coatings on the copper selenide nanowires had lost their aromaticity (Supporting Information Figure S3b,c). In addition, analysis by electron energy-loss spectroscopy of the carbon K edge performed using a STEM suggested that the polymer coatings have a similar chemical state as the amorphous carbon coating after the thermal purification process (Supporting Information Figure S10). The purified product potentially consists of a mixture of three different phases of copper selenide. These phases are hexagonal (CuSe, PDF no. 01-072-8417 34-171), orthorhombic (CuSe, PDF no. 86-1239), and cubic (Cu_2Se, PDF no. 46-1129) copper selenide (Supporting Information Figure S11). The thermally purified copper selenide nanowires are polycrystalline with an average domain size of 23 ± 13 nm, as approximated from the XRD data (Figure 3) using the Scherrer equation.[40] In addition, HAADF-STEM images of the purified copper selenide nanowires (Supporting Information Figure S9) indicate that the anisotropic nanostructure remains intact after thermal treatment to selectively remove the unreacted selenium nanowire template.

Optoelectronic properties of selenium nanowires and purified copper selenide@polystyrene nanowires were characterized using UV−vis spectroscopy. Both materials have electronic transitions that can be excited in the UV−vis region of the electromagnetic spectrum. The UV−vis absorption spectrum of selenium nanowires (Figure 4a) spans from the UV to the near infrared (NIR) wavelengths of the electromagnetic spectrum, with three strongly absorbing peaks at 344, 437, and 559 nm, respectively. These peaks represent intramolecular and intermolecular electronic transitions.[41] The absorption spectrum of copper selenide (Figure 4b) indicates that the material can absorb a wide range of the photon energies, but it is most efficient at absorbing in the UV region of the electromagnetic spectrum. The purified CuSe-Cu_2Se@PS nanowires have an absorption edge at 508 nm (2.44 eV) that corresponds to the direct bandgap energy. The bandgap energy falls in between that of the reported values of cubic (2.2 eV)[6] and hexagonal (2.0 and 2.8 eV)[9] copper selenide. The observed bandgap might be due to mixing of the bandgaps of the two different phases.

The inset plots of Figure 4a and b are used to estimate the indirect bandgap of the selenium and copper selenide nanowires using the formula $(\alpha h\nu)^{1/2} = (Ah\nu/l)^{1/2} = (h\nu - E_g)$.[6] The absorption coefficient (α) can be calculated using the

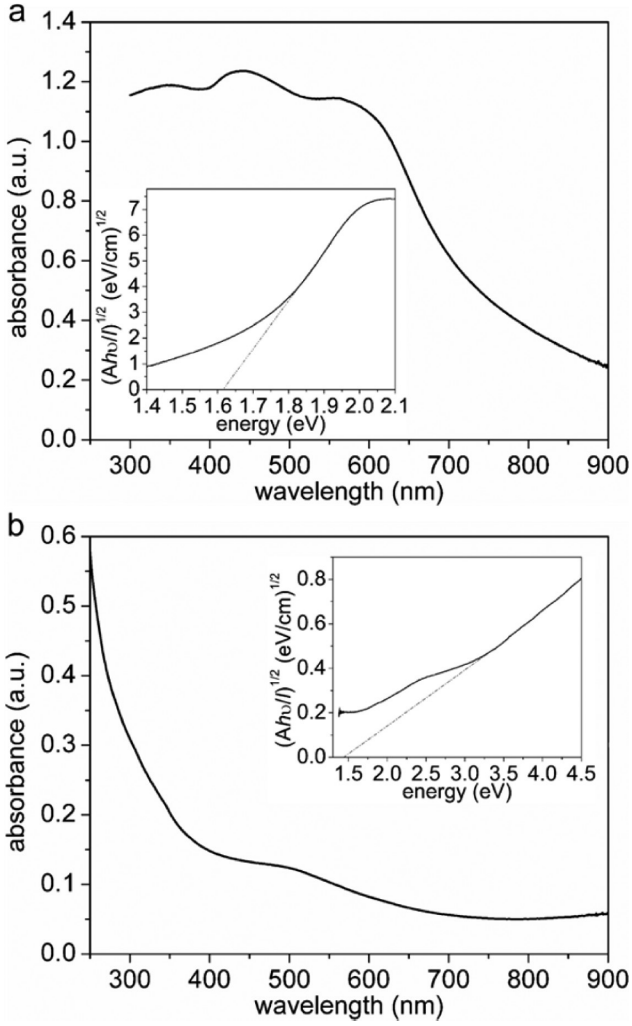

Figure 4. UV−vis absorption studies conducted on uniform dispersions of (a) selenium nanowires and (b) copper selenide@polystyrene nanowires (purified by heat treatment) as well as the corresponding plots used to estimate the indirect bandgap of each sample (a and b insets, respectively).

Beer−Lambert equation from acquired absorbance (A) values and the known light path length (l). At the corresponding spectral wavelengths, the photon energy is calculated by multiplying frequency (ν) of the wavelength of radiation by the Planck constant (h). The bandgap energy (E_g) of the material is estimated by determining the x intercept of the steepest slope in a plot of $(Ah\nu/l)^{1/2}$ against $h\nu$. The estimated indirect bandgap of the selenium nanowires with an average diameter of 29 ± 9 nm is 1.61 eV, which closely matches the value of 1.65 eV previously reported on nanowires of a similar diameter.[41] The purified CuSe-Cu_2Se@PS nanowires have has an indirect bandgap energy of 1.44 eV that is similar to reported literature values of 1.0−1.4 eV.[42]

CONCLUSIONS

This Article is the first report of the direct conversion of selenium nanowires into cuprous and cupric selenide@polystyrene nanowires. This study demonstrated that the transformation of selenium to copper selenide proceeds readily under ambient conditions. The reaction is initiated by the surface-initiated atom transfer radical polymerization of styrene on the surfaces of the selenium nanowires or Cu/CuOx

substrate. It is proposed that the styrene radical or polystyrene radicals subsequently reduced the Cu(II) oxide species to Cu(I) analogues and Cu(0). These copper species subsequently react either through an electrochemical or a solid-state process with the selenium nanowires. The single crystalline selenium nanowire templates were simultaneously converted into polycrystalline cuprous and cupric selenide nanowires encapsulated with a thin sheath of polystyrene. Transformation from single crystalline selenium templates into polycrystalline copper selenide@polystyrene nanowires was accompanied with an increase in the diameter of the copper selenide nanowires. These polycrystalline copper selenide nanowires coated with a thin sheath of polystyrene have an average composition of Cu1.75±0.04Se@PS, as determined by EDS analysis on a collection of the nanostructures. Spot EDS analyses performed along the length of individual Cu1.75±0.04Se@PS nanowire revealed a larger variation in Cu and Se composition, which could be due to the formation of the polystyrene layer that impedes the selenium nanowires from reacting uniformly with the Cu(I) species and prevents uniform physical contact between the selenium nanowires and the Cu/CuOx substrate required for a solid-state reaction. The as-synthesized product was purified by selectively removing the unreacted selenium nanowires (~3% impurity) through a process of selective thermal evaporation that also transformed the polystyrene to an encapsulating layer of amorphous carbon. The purified CuSe-Cu_2Se@PS nanowires exhibited an indirect bandgap of 1.44 eV. This process could be readily extended to the formation and polymer encapsulation of other copper selenide nanostructures, but it may be adapted for the polymer encapsulation of other nanostructures.

■ ASSOCIATED CONTENT

Supporting Information

X-ray photoelectron spectroscopy and electron energy-loss spectroscopy analysis of copper selenide@polystyrene nanowires. Quantitative Rietveld refinements for the powder XRD of the crude and thermally purified copper selenide@polystyrene nanowires. Electron microscopy images of copper selenide@polystyrene nanowires post thermal treatment. This material is available free of charge via the Internet at http://pubs.acs.org.

■ AUTHOR INFORMATION

Corresponding Author

*E-mail: bgates@sfu.ca.; Tel: 778 782 8066; Fax: (+1) 778 782 3765.

Notes

The authors declare no competing financial interest.

■ ACKNOWLEDGMENTS

This research was supported in part by the Natural Sciences and Engineering Research Council (NSERC) of Canada, the Canada Research Chairs Program (to B.D. Gates), and Simon Fraser University (Graduate Fellowship for M.C.P. Wang). This work made use of the 4D LABS shared facilities supported by the Canada Foundation for Innovation (CFI), British Columbia Knowledge Development Fund (BCKDF), Western Economic Diversification Canada, and Simon Fraser University.

■ REFERENCES

(1) Xu, J.; Zhang, W. X.; Yang, Z. H.; Ding, S. X.; Zeng, C. Y.; Chen, L. L.; Wang, Q.; Yang, S. H. *Adv. Funct. Mater.* **2009**, *19*, 1759−1766.
(2) Zhang, Y.; Hu, C. G.; Zheng, C. H.; Xi, Y.; Wan, B. Y. *J. Phys. Chem. C* **2010**, *114*, 14849−14853.
(3) Zolotovskaya, S. A.; Posnov, N. N.; Prokosin, P. V.; Yumashev, K. V.; Gurin, V. S.; Alexeenko, A. A. *Semiconductors* **2004**, *38*, 812−817.
(4) Hessel, C. M.; Pattani, V. P.; Rasch, M.; Panthani, M. G.; Koo, B.; Tunnell, J. W.; Korgel, B. A. *Nano Lett.* **2011**, *11*, 2560−2566.
(5) Okimura, H.; Matsumae, T.; Makabe, R. *Thin Solid Films* **1980**, *71*, 53−59.
(6) Choi, J.; Kang, N.; Yang, H. Y.; Kim, H. J.; Son, S. U. *Chem. Mater.* **2010**, *22*, 3586−3588.
(7) Deka, S.; Genovese, A.; Zhang, Y.; Miszta, K.; Bertoni, G.; Krahne, R.; Giannini, C.; Manna, L. *J. Am. Chem. Soc.* **2010**, *132*, 8912−8914.
(8) Deng, Z. T.; Mansuripur, M.; Muscat, A. J. *J. Mater. Chem.* **2009**, *19*, 6201−6206.
(9) Hsu, Y. J.; Hung, C. M.; Lin, Y. F.; Liaw, B. J.; Lobana, T. S.; Lu, S. Y.; Liu, C. W. *Chem. Mater.* **2006**, *18*, 3323−3329.
(10) Jagminas, A.; Juskenas, R.; Gailiute, I.; Statkute, G.; Tomasiunas, R. *J. Cryst. Growth* **2006**, *294*, 343−348.
(11) Li, D. P.; Zheng, Z.; Lei, Y.; Ge, S. X.; Zhang, Y. D.; Zhang, Y. G.; Wong, K. W.; Yang, F. L.; Lau, W. M. *CrystEngComm* **2010**, *12*, 1856−1861.
(12) Son, D. H.; Hughes, S. M.; Yin, Y.; Alivisatos, A. P. *Science* **2004**, *306*, 1009−1012.
(13) Statkute, G.; Tomasiunas, R. *J. Appl. Phys.* **2007**, *101*, 113715−1-113715-9.
(14) Vinod, T. P.; Jin, X.; Kim, J. *Mater. Res. Bull.* **2011**, *46*, 340−344.
(15) Yu, R.; Ren, T.; Sun, K. J.; Feng, Z. C.; Li, G. N.; Li, C. *J. Phys. Chem. C* **2009**, *113*, 10833−10837.
(16) Zhang, S. Y.; Fang, C. X.; Tian, Y. P.; Zhu, K. R.; Jin, B. K.; Shen, Y. H.; Yang, J. X. *Cryst. Growth Des.* **2006**, *6*, 2809−2813.
(17) Chen, H. H.; Zou, R. J.; Wang, N.; Zhang, Z. Y.; Sun, Y. G.; Yu, L.; Tian, Q. W.; Chen, Z. G.; Hu, J. Q. *J. Mater. Chem.* **2011**, *21*, 3053−3059.
(18) Kemell, M.; Ritala, M.; Leskela, M. *Crit. Rev. Solid State Mater. Sci.* **2005**, *30*, 1−31.
(19) Panthani, M. G.; Akhavan, V.; Goodfellow, B.; Schmidtke, J. P.; Dunn, L.; Dodabalapur, A.; Barbara, P. F.; Korgel, B. A. *J. Am. Chem. Soc.* **2008**, *130*, 16770−16777.
(20) George, S.; Xia, T. A.; Rallo, R.; Zhao, Y.; Ji, Z. X.; Lin, S. J.; Wang, X.; Zhang, H. Y.; France, B.; Schoenfeld, D.; Damoiseaux, R.; Liu, R.; Lin, S.; Bradley, K. A.; Cohen, Y.; Nal, A. E. *ACS Nano* **2011**, *5*, 1805−1817.
(21) Wang, M. C. P.; Gates, B. D. *Chem. Commun.* **2012**, *48*, 8589−8591.
(22) Morikawa, H. *Jpn. J. Appl. Phys.* **1970**, *9*, 607−614.
(23) Kaito, C. *J. Cryst. Growth* **1974**, *24*, 563−567.
(24) Shiojiri, M.; Kaito, C.; Saito, Y.; Teranishi, K.; Sekimoto, S. *J. Cryst. Growth* **1981**, *52*, 883−886.
(25) Hirota, Y.; Isshiki, T.; Okashita, K.; Shiojiri, M. *J. Cryst. Growth* **1991**, *112*, 55−70.
(26) Kaito, C.; Nonaka, A.; Kimura, S.; Suzuki, N.; Saito, Y. *J. Cryst. Growth* **1998**, *186*, 386−392.
(27) Ouchi, A.; Bastl, Z.; Bohacek, J.; Orita, H.; Miyazaki, K.; Miyashita, S.; Bezdicka, P.; Pola, J. *Chem. Mater.* **2004**, *16*, 3439−3445.
(28) Ishikawa, Y.; Kido, O.; Kimura, Y.; Kurumada, M.; Suzuki, H.; Saito, Y.; Kaito, C. *Surf. Sci.* **2004**, *548*, 276−280.
(29) Chen, J. Y.; Wiley, B. J.; Xia, Y. *Langmuir* **2007**, *23*, 4120−4129.
(30) Huang, X. H.; Neretina, S.; El-Sayed, M. A. *Adv. Mater.* **2009**, *21*, 4880−4910.
(31) Allcock, H. R.; Lampe, F. W.; Mark, J. E. *Contemporary Polymer Chemistry*; Prentice Hall: Upper Saddle River, NJ, 2003.
(32) Bai, Y.; Rong, F. X.; Wang, H.; Zhou, Y. H.; Xie, X. Y.; Teng, J. W. *J. Chem. Eng. Data* **2011**, *56*, 2563−2568.
(33) Lock, E. H.; Petrovykh, D. Y.; Mack, P.; Carney, T.; White, R. G.; Walton, S. G.; Fernsler, R. F. *Langmuir* **2010**, *26*, 8857−8868.

(34) Gates, B.; Mayers, B.; Wu, Y. Y.; Sun, Y. G.; Cattle, B.; Yang, P.; Xia, Y. *Adv. Funct. Mater.* **2002**, *12*, 679−686.
(35) Bish, D. L.; Howard, S. A. *J. Appl. Crystallogr.* **1988**, *21*, 86−91.
(36) Jeong, U. Y.; Herricks, T.; Shahar, E.; Xia, Y. *J. Am. Chem. Soc.* **2005**, *127*, 1098−1099.
(37) Chen, Y. W.; Li, L.; D'Ulivo, A.; Belzile, N. *Anal. Chim. Acta.* **2006**, *577*, 126−133.
(38) Chen, Z. X.; Shen, Y. H.; Xie, A. J.; Zhu, J. M.; Wu, Z. F.; Huang, F. Z. *Cryst. Growth Des.* **2009**, *9*, 1327−1333.
(39) El-Salmawi, K.; Abu Zeid, M. M.; El-Naggar, A. M.; Mamdouh, M. *J. Appl. Polym. Sci.* **1999**, *72*, 509−520.
(40) Patterson, A. L. *Phys. Rev.* **1939**, *56*, 978−982.
(41) Gates, B.; Mayers, B.; Cattle, B.; Xia, Y. *Adv. Funct. Mater.* **2002**, *12*, 219−227.
(42) Omadelung, O.; Schulz, M.; Weiss, H. *Landolt-Borstein - Group III Condensed Matter Numerical Data and Functional Relationships in Science and Technology*; Springer-Verlag: Berlin, 1998; Vol. *III/17E-17F-41C*.